energies

MDPI

Article

Comparison of Molten Salts and Thermal Oil in Parabolic Trough Power Plants for Different Sites and Different Storage Capacities

Jürgen Dersch [1,*], Michael Karl Wittmann [2] and Tobias Hirsch [2]

[1] German Aerospace Center (DLR e.V.), Linder Höhe, 51147 Cologne, Germany
[2] German Aerospace Center (DLR e.V.), Pfaffenwaldring 38-40, 70569 Stuttgart, Germany; michael.wittmann@dlr.de (M.K.W.); tobias.hirsch@dlr.de (T.H.)
* Correspondence: juergen.dersch@dlr.de; Tel.: +49-2203-6012219

Abstract: This study compares the levelized cost of energy (LCOE) of parabolic trough solar power plants using thermal oil or two different molten salt mixtures located at three different sites and with different thermal storage capacities. The necessity of using appropriate model approaches for the temperatures along a loop of the solar field is discussed, as well as the utilization of heat from thermal storage for freeze protection of the molten salt plants. The ternary salt mixture with a lower temperature limit of 170 °C and an upper temperature limit of 500 °C shows the lowest LCOE for all sites and almost all investigated storage capacities. Molten salts as heat transfer fluids are particularly favorable for sites with high irradiation and plants with large storage capacities of more than six full load hours.

Keywords: parabolic trough; molten salt; levelized cost of energy; freeze protection

Academic Editors: Fabio Montagnaro and Roberto Solimene

Received: 25 November 2024
Revised: 30 December 2024
Accepted: 3 January 2025
Published: 13 January 2025

Citation: Dersch, J.; Wittmann, M.K.; Hirsch, T. Comparison of Molten Salts and Thermal Oil in Parabolic Trough Power Plants for Different Sites and Different Storage Capacities. *Energies* **2025**, *18*, 326. https://doi.org/10.3390/en18020326

1. Introduction

Parabolic trough solar thermal power plants collect solar energy by using large collectors which consist of parabolic-shaped mirrors concentrating the incoming direct irradiation from the sun onto a linear receiver which is located in the focal line of the parabola. These receivers convert the concentrated radiation into thermal energy. A heat transfer fluid (HTF) is pumped through them to transport the heat from the solar field to the power block, where it is used to generate electricity. Almost all existing commercial plants are using Rankine cycle power blocks, with steam generators heated by the HTF. Most of today's parabolic trough power plants are using thermal oil as HTF, which limits the maximum operating temperature to 400 °C due to the thermal stability of this oil. Many of these plants have a two-tank molten salt storage to provide dispatchability, and the storage medium is typically Solar Salt, a mixture of KNO_3-$NaNO_3$ (40–60 wt%). This storage fluid can be used up to 565° or even at higher temperatures. Kearney et al. [1] were some of the first to proposed the use of Solar Salt also as a heat transfer medium in the solar field in order to make use of the full temperature potential of the storage medium, omit oil/salt heat exchangers, and use power blocks with higher live steam conditions and thus higher efficiencies.

In opposition to these clear advantages, molten salts show increased melting temperatures, which complicates the operation of large distributed piping networks like those in parabolic trough solar fields, since solidification must be avoided under any circumstances and freeze protection becomes an important issue. The first demonstration and pilot plants have been built, e.g., the Archimede plant [2] in Sicily and the Evora Molten Salt

Platform [3,4] in Portugal. In China, a 50 MW commercial power plant has been operating since 2020 [5].

Several studies have dealt with the advantage of parabolic trough plants using molten salt as HTF and storage medium. Many of these studies consider Solar Salt, e.g., [1,6–8], since this HTF has been used in solar tower plants and, therefore, the physical properties are well investigated. Solar Salt freezes at about 220–240 °C and thus requires additional effort for freeze protection.

Other salt mixtures show lower melting temperatures, but often their upper temperature limit is also lower. Giaconia et al. [9] have considered different synthetic oils and different molten salt mixtures, including the ternary salt ($Ca(NO_3)_2$-KNO_3-$NaNO_3$, 42–43–15 wt.%, commercial names: Hitec XL or YaraMOST) and have found that this mixture shows a lower levelized cost of energy (LCOE) compared to synthetic oil and Solar Salt. Their study was made for a site in Italy, and the temperature range of the ternary salt was limited to 250–425 °C. The lower limit was set by the authors due to increasing viscosity for this HTF at lower temperatures, while the upper limit was set due to stability reasons.

Delise et al. [10] considered Hitec XL as HTF and storage medium in a study simulating a 50 MW CST plant with 7.5 h of TES in Sicily. They showed that this HTF can provide lower LCOE compared to plants using Solar Salt or thermal oil as HTF, although they have limited the temperature range for Hitec XL to 250–450 °C. They did not consider different storage capacities or different sites.

Starke et al. [11] compared several high-temperature molten salts, optimized the plant configuration, and considered increased costs for corrosive salt mixtures for a site in Chile. They reported an optimal field outlet temperature of about 520 °C for molten salt parabolic trough plants.

Gallardo et al. [12] published a paper comparing Solar Salt and Hitec XL salt for a site in Portugal and found an increased net electrical output of about 50% for Hitec XL. They only considered a TES capacity of 7.5 h.

Fahir et al. [13] investigated nine different HTFs (only four of them with maximal operating temperatures of 400 °C or above) in a 50 MW CST plant using Linear Fresnel collectors for several sites, all of them in Pakistan.

Kannaiyan and Bokde [14] compared the performance of parabolic trough collector fields using VP1, Solar Salt, and water as HTFs. Their focus was on operational control, and they did not compute annual performance.

Many recent studies consider PV-CSP hybrid solar power plants, e.g., [15–17], which promise lower LCOE compared to standalone concentrating solar thermal (CST) plants; but for these hybrid plants, the LCOE is a kind of blended value. This paper is focused on the CST plants. Some of the studies on hybrid plants consider supercritical CO_2 power cycles instead of Rankine cycles [18–20], which may offer additional cost benefits, but they are not state-of-the-art technology today.

The goal of this study is to investigate the impact of different storage capacities, different solar resources, and different latitudes on LCOE of solar thermal power plants using three different HTFs: thermal oil (commercial name: VP1), Solar Salt, and a ternary salt (commercial name: YaraMOST). This study is based on annual performance calculations of parabolic trough plants with a fixed power block size of 160 MW gross electrical output. Thermal storage capacity varied from 6 to 18 full load hours, and the solar field sizes offering the lowest LCOE for each site, TES sizes, and HTFs were retrieved. The overall goal is to find out which of these HTFs would be most suitable for which site and TES size. Furthermore, the importance of considering suitable modeling approaches for the representative solar field temperature and freeze protection is discussed.

2. Methodology

2.1. Software Tool

The software tool greenius has been used in this study for the techno-economic evaluation of parabolic trough plants using VP1, Solar Salt, and YaraMOST at different sites and with different storage capacities. This software tool is developed for several years at DLR and it is available for free from [21]. On this website, detailed information is given about the software. For the current study, greenius was modified in order to simulate freeze protection using primarily heat from the thermal storage system and minimize freeze protection from auxiliary heaters, which may be fired with natural gas or a green fuel. Using storage heat should be the preferred freeze protection mode, since using natural gas would considerably increase the CO_2 emissions of the CST plant and using a green fuel would be more expensive. Freeze protection by electrical heating would also be more expensive for most sites. This can be illustrated by a simple calculation, assuming a net efficiency of 38% for the conversion of heat to electricity and a LCOE of 0.12 EUR/kWh. With these assumptions, the heat stored in the molten salt tanks would be worth 0.046 EUR/kWh, which is considerably cheaper than electricity and also cheaper than green fuels.

The software tool greenius offers two different simulation approaches for parabolic trough solar fields: a simple model using the arithmetic mean temperature between solar field inlet and outlet temperatures for heat loss calculations, and an advanced model using a spatial discretization of the representative loop with local temperatures and individual heat loss calculation for each section. The advanced model was originally developed to simulate direct steam generation in parabolic trough fields, but can also be used for single-phase fluids. During our study, we found that the simple model, using just the arithmetic mean temperature, would underestimate the thermal losses and thus overestimate the net heat output of the solar field considerably for the molten salt configurations.

Figure 1 shows the extend of heat loss underestimation for the three HTFs considered here. The heat losses in the absorber tubes (also called heat-collecting elements, HCE) are highly nonlinear depending on the absorber temperature. Thus, higher temperatures and larger temperature spreads between the inlet and outlet of the solar field amplify this effect. The graph was generated using 12 elements along one loop, the same discretization as used in greenius. Using 40 elements instead only changed the results by less than 0.4%; therefore, the annual yield simulations were performed with 12 elements in order to limit the computation time. The highest deviation between the simple and the spatially discretized model in heat loss calculation is observed for Solar Salt, while for VP1, the error is much lower. For the design irradiation of 850 W/m², the ratios are 1.18 (Solar Salt), 1.10 (YaraMOST), and 1.03 (VP1). Furthermore, the relative error increases with lower irradiation (lower thermal input) for the molten salts, while it is almost independent from the irradiation for VP1.

This effect can be explained by the increasing impact of the heat losses compared to the incoming heat and the changing temperature profile along the loop for lower irradiance (Figure 2). The higher the overall operating temperature (e.g., with Solar Salt), the more pronounced this effect. The impact of these differences in heat loss calculation on the annual yield and LCOE is discussed in Section 3.

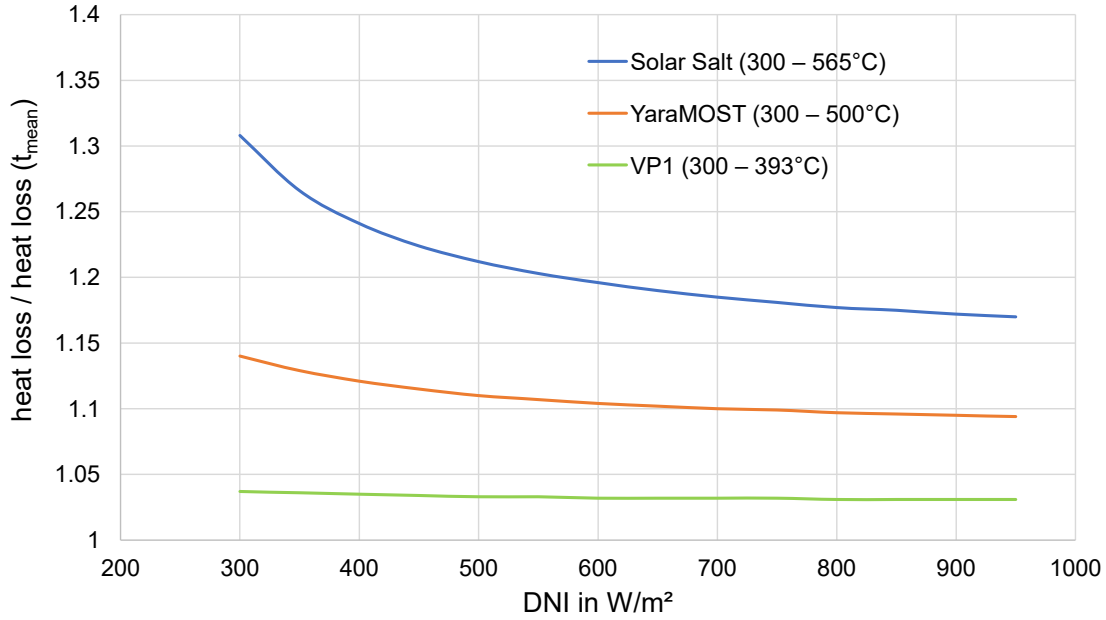

Figure 1. Relative heat losses of a single loop calculated using spatially discretized temperatures divided by the heat loses calculated using the arithmetic mean temperature for different heat transfer fluids.

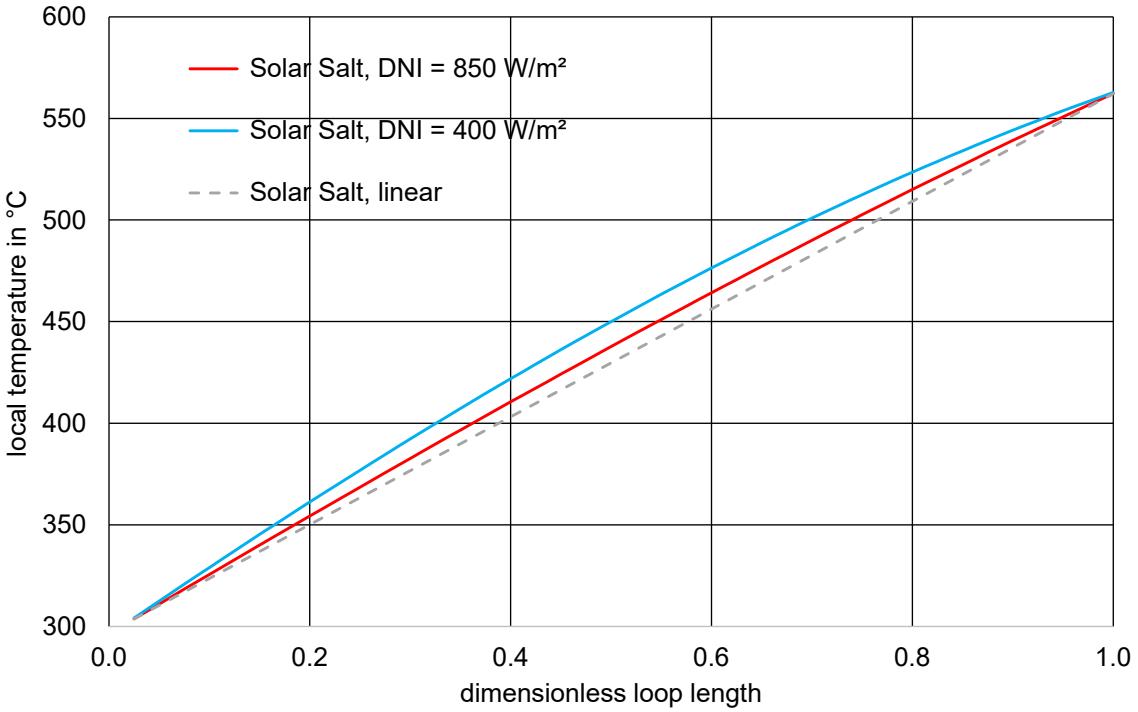

Figure 2. Calculated temperature profile along the loop for a plant using Solar Salt for different direct normal irradiance (DNI) values, compared to a linear temperature profile.

2.2. Plant Design

For the different HTFs, the power plants' principle layouts are different. While CST plants using thermal oil as HTF need heat exchangers between the storage tanks and the oil cycle, plants using molten salts are simpler and do not need this heat exchanger. During their normal operation mode, HTF is drawn from the cold salt tank, pumped through the solar field, heated up to the nominal outlet temperature, and stored in the hot tank. The schematic drawings in Figure 3 are simplified in the sense that they do not show all

interconnecting and bypass pipes necessary in the power plants for start-up and freeze protection operation.

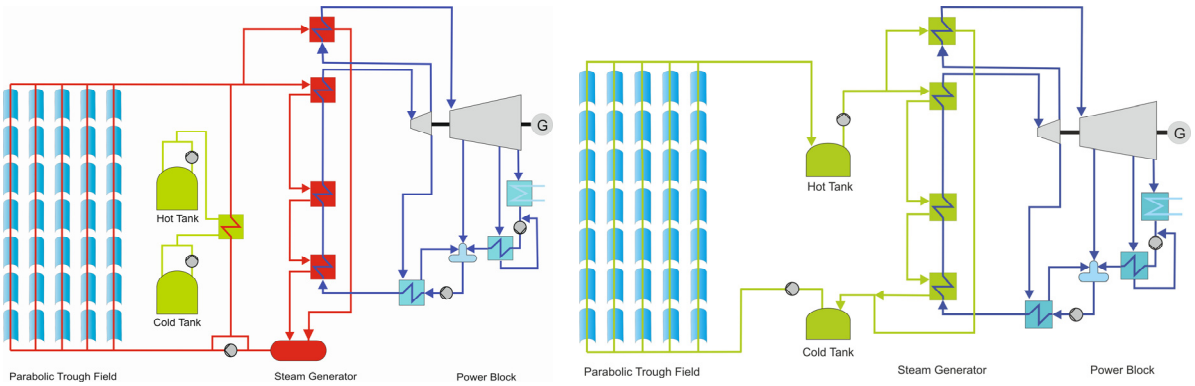

Figure 3. (**a**) Scheme of the parabolic trough plant using thermal oil as HTF; (**b**) scheme of the plant using molten salt as HTF. (red lines: VP1, green lines molten salt, blue lines: water/steam).

For all plants the same type of parabolic trough collector has been assumed: the Heliotrough collector developed by TSK Flagsol [22]. This is a large aperture collector with 193m length and 6.77 m of aperture width. For the solar field layout, designers have several degrees of freedom: the number of collectors forming a loop can be varied and the HCE or absorber tube diameters can be adapted (see Section 2.3 for more details). Pressure loss over each loop must also be considered in order to keep the required pumping power and the maximum pressure in the solar field within a reasonable range. Preliminary design calculations have been made and, as a result, the thermal oil plants are simulated assuming 89 mm HCEs and 4 collectors per loop, while the molten salt plants have 80 mm HCEs and 6 collectors per loop. More design details are given in Table 1.

It has been assumed that the plants are operating in solar driven mode, which means that they start in the morning after sunrise. The solar field is heated up and the power block starts as soon as the solar field delivers sufficient heat. When the power block runs at full load, the excess heat produced by the solar field is stored in the molten salt tanks and used to run the power block after sunset with full load. When the storage is empty, the power block is shut down and the cycle starts again the next morning. After sunset, the solar field is assumed to run in recirculation mode and cools down. The temperature does not fall immediately, but, due to the large thermal inertia of the system, there is a kind of exponential temperature decay. Once the calculated solar field temperature reaches the freeze protection temperature, external heat is supplied to keep the system above this temperature limit.

For the molten salt plants, a certain amount of heat is kept in the thermal storage to facilitate freeze protection. The total amount of heat needed for the next night is calculated in a preprocessing model run. This heat, required for freeze protection during the following night, cannot be used for electricity production, but will be reserved for this purpose.

Extended forecasting might be used in order to increase freeze protection from storage for longer periods with low irradiation, but this was not considered here. The expected impact of this measure is small, since freeze protection using external heat is typically required after days with poor irradiation. Freeze protection from external heat is modeled by calculating the heat required to keep the solar field outlet temperature above the freeze protection temperature. This amount of heat is used to calculate the natural gas demand (using a heater efficiency 90%) and finally to calculate operating costs for the gas demand. Additional electrical freeze protection was not considered in the model.

Table 1. Major design parameters of the three different parabolic trough plants (SF: solar field).

Parameter	VP1 Plant	YaraMOST Plant	Solar Salt Plant	Unit
Collector net aperture area		1283		m²
Collector aperture width		6.77		m
Collector length		193		m
HCE diameter (outer)	89	80	80	mm
No. of collectors per loop	4	6	6	-
Mean cleanliness		97		%
Row distance		21		m
Optical peak efficiency	81.6	81.2	81.2	%
Nom. SF inlet temperature	298	300	300	°C
Nom. SF outlet temperature	393	500	565	°C
Nom. Field pressure drop	12	14	18	bar
Spec. heat losses of field piping	0.0163	0.0165	0.0167	W/(m²K)
Minimum temperature	60	170	270	°C
Availability		99		%
Power block gross output		160		MW
Nominal power block efficiency	39.0	44.0	46.5	%
Condenser type		ACC		
Storage medium	Solar Salt	YaraMOST	Solar Salt	
Storage heat losses	1.0	1.3	1.5	%/day

Molten salt physical properties and temperature limits have been taken from Bonk [23]. Solar field size, determined by the number of parallel loops, has been optimized for each site, storage capacity, and HTF by searching for the configuration which gives the lowest LCOE in each individual case. This was performed using a systematic parameter variation.

2.3. Absorber Diameter and Heat Losses

Absorber heat losses are the most important loss mechanism for these plants, and design measures can be taken to minimize these heat losses. Higher concentration ratios can be used to minimize HCE heat losses, and they may be reached by using smaller HCE diameters for a collector with given aperture width. Riffelmann [24] published a study considering different HCE diameters for the Ultimate Trough collector, and he showed that the smaller HCE might offer advantages for molten salt trough fields. There is a trade-off between maximizing the intercept factor and minimizing thermal losses. A larger HCE diameter would increase the intercept factor (which has an impact on optical design efficiency), but would also increase heat losses of the HCE, while a smaller diameter decreases both parameters.

Heat loss measurements or publications from manufacturers of HCEs with different diameters and for the required temperature ranges are rarely available. NREL [25] has published measurements for Schott PTR70 Receivers, and the authors of this study have undisclosed measurements and approximations for 2 other HCEs with 70 mm outer diameter. Heat losses are proportional to the absorber surface; thus, they can approximately be scaled using the ratio of absorber tube diameters. NREL has measured PTR70 heat losses up to 509 °C, although this specific receiver was not made for long term utilization at such

high temperatures. The other HCEs shown in Figure 4 are explicitly designed for molten salt plants. In this study, the heat loss correlation for the receiver called "Molten salt HCE 2" was used. It shows the highest heat losses of the three HCE types in Figure 4, but gives reasonable values for temperatures below 250°, in contrast to "Molten salt HCE 1".

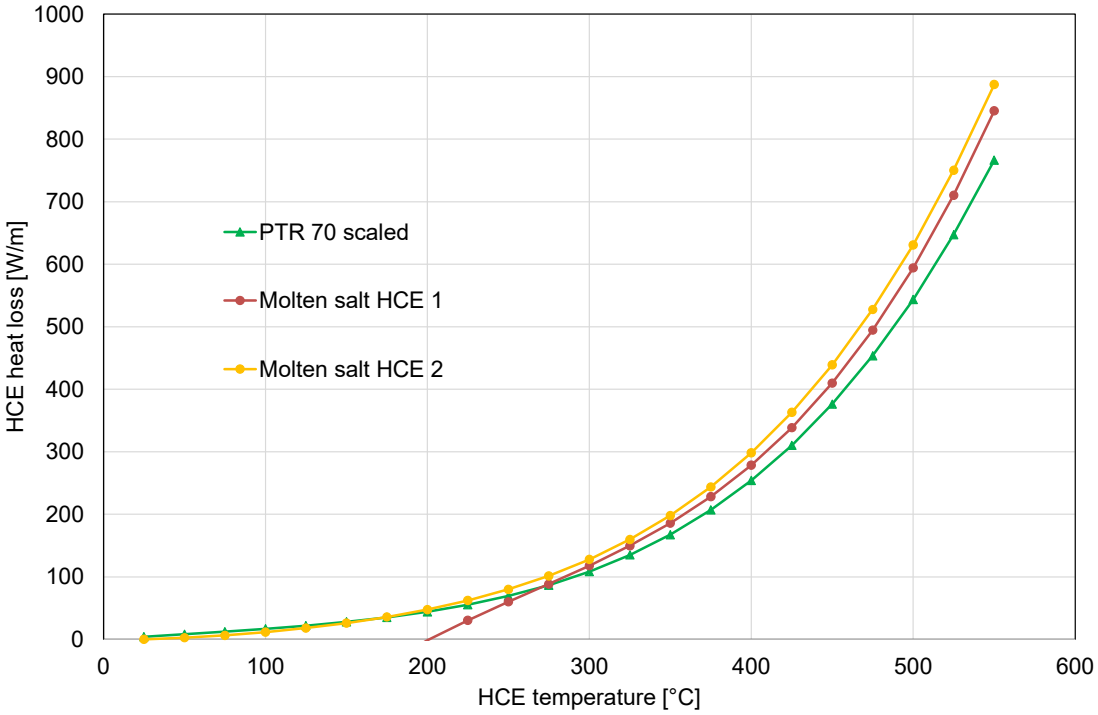

Figure 4. HCE heat losses from different sources scaled to a 80 mm diameter receiver. For molten salt, HCE 2 is used in this study due to conservative assumptions and consistent heat losses at lower temperatures.

Calculations have shown that 80 mm HCEs offer reduced heat losses compared to 89 mm HCEs by approximately 10% for Solar Salt, while the optical efficiency is only reduced by less than 1%. This leads to an overall efficiency increase of about 1.6 percent points for the Solar Salt system with 80 mm HCEs, while the overall efficiency of the VP1 system is almost unaffected. Therefore, the simulations were performed assuming Heliotrough collectors with 89 mm HCEs for the VP1 systems and with 80 mm HCEs for the molten salt systems.

2.4. Characterization of the Different Sites

It is well known that solar resource (DNI) and site latitude have a considerable impact on design, annual yield, and LCOE of CST power plants. Therefore, 3 different sites have been considered in this study: Ouarzazate (Morocco), representing a north African site with good solar conditions; Saih Al-Dahal (Dubai), representing a site with lower solar resource, but closer to the equator; and Murcia (Spain), with almost the same solar resource as Saih Al-Dahal, but located in southern Europe. The first two locations are known as sites hosting large CST plants, and the third site was chosen to investigate the impact of latitude.

Table 2 shows those parameters which are of importance for the annual performance of CST plants. Global horizontal irradiance (GHI) is also shown, although CST plants can only use DNI.

Table 2. Parameters characterizing the 3 sites considered in this study.

Site Parameter	Ouarzazate Morocco	Saih Al-Dahal Dubai	Murcia Spain	Unit
Latitude	30.9	24.8	38.0	°N
Annual DNI	2518	2026	2020	kWh/m²
Mean temperature	18.8	28.4	18.8	°C
Min/max temperature	−0.3/38.9	9.6/47.3	0.5/40.7	°C

2.5. System Costs

For the economic comparison of different plants and sites, component costs and other financial conditions must be known in order to calculate LCOE according to the following formula:

$$\text{LCOE} = \frac{\text{Total Investment Costs} + \sum_{t=1}^{t_{ges}} \frac{\text{Annual Running Costs}_t}{(1+r)^t}}{\sum_{t=1}^{t_{ges}} \frac{\text{Annual Electrical Yield}_t \times (1-d)^{t-1}}{(1+r)^t}}, \quad (1)$$

where r is the interest rate, t is the year within the period of use (1, 2, … t_{ges}), t_{ges} is the system life time in years, and d is the yearly degradation rate.

Cost assumptions (see Table 3) have been taken from the internal cost database at the DLR Institute of Solar Research. This database uses publicly available information as well as non-disclosed information from industry partners to come to reasonable cost assumptions. Specific costs for thermal storage systems have been calculated based on detailed information gained from [26]. Specific solar field costs of the molten salt plants are assumed to be 10% above the cost for the VP1 solar field. They need no heat exchangers between the oil and molten salt cycles and no HTF ullage system, but the higher outlet temperatures require higher grade steel specimens for the piping, which are more expensive. Similar considerations were made for power block costs.

Table 3. Cost assumptions and financial parameters (operation and maintenance: O&M; erection, procurement, commissioning: EPC).

Component	Unit	VP1 Plant	YaraMost Plant	Solar Salt Plant
Solar field cost	€/m²	205	225	225
Power block cost	€/kW$_e$	1000	1100	1100
TES cost	€/kWh$_{th}$	47	24	19
Land cost	€/m²		1.0	
Surcharge for EPC, etc.	%		20	
Interest rate	%/a		6.0	
Lifetime	a		25	
Annual degradation	%		0.4	
Annual O&M costs	%		2	
Fuel costs	€/kWh$_{th}$		0.06	
Annual insurance costs	%		0.7	

It should be mentioned that these cost assumptions are based on pre-COVID-19 data, and costs have considerably increased since then. On the other hand, almost no new projects have been published and available data are rare. The goal of this study was rather a comparison between different HTFs, and therefore the cost assumptions were not changed.

Multiplying all component costs with the same inflation factor would increase LCOE, but would not change the overall outcome of the study.

3. Results

Figure 5 shows the results of the simulation study for all sites, HTFs, and storage capacities. The lowest LCOE values are reached for the site in Morocco, which offers the highest solar resource. This is an expected result, since DNI is known as the most important parameter for LCOE of CST systems. This figure also shows the considerable impact of latitude, since the LCOE for Dubai are lower than those for Spain, although both sites have almost the same annual sum of DNI. This can be explained by the lower seasonality effects of sites closer to the equator. The installed equipment is utilized better throughout the year. Plants using YaraMOST show the lowest LCOE for all sites and almost all considered storage capacities. Only for 6 h of TES capacity at the sites in Spain and Dubai, VP1 reach the same LCOE, and, for 18 h, TES capacity in Morocco Solar Salt is equivalent to YaraMOST.

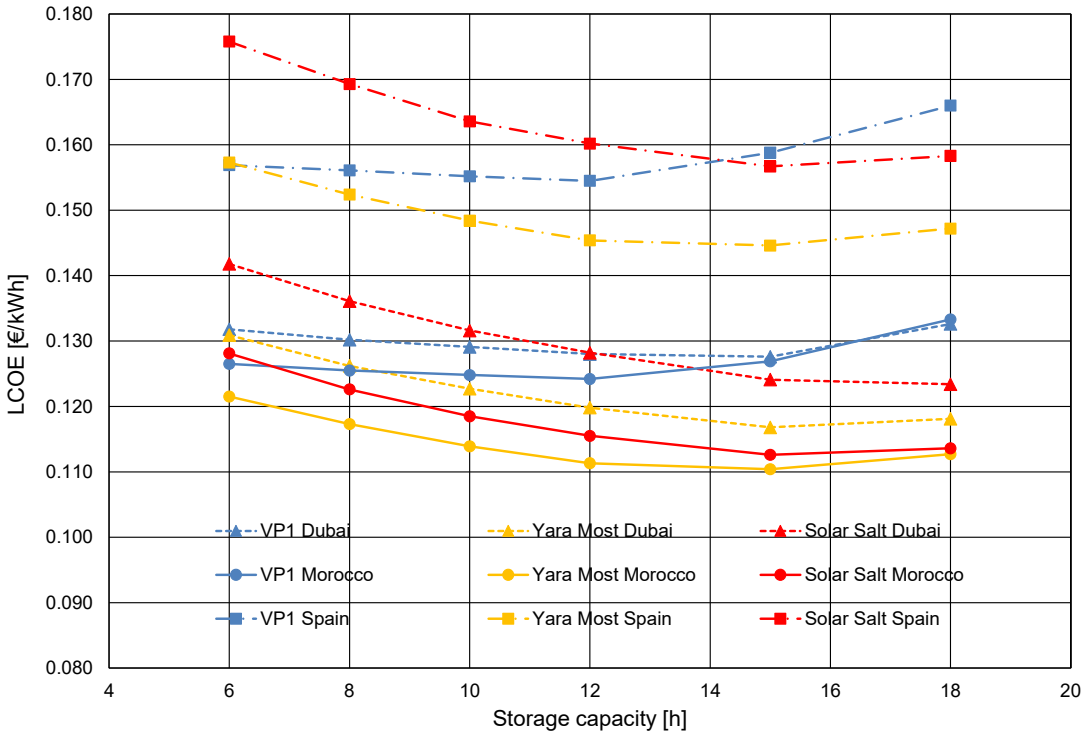

Figure 5. Results showing the least LCOE configurations for each site, HTF, and storage capacity.

Molten salt plants tend to have lower LCOE compared to thermal oil plants, particularly for large storage capacities and high annual DNI. For small storage capacities of about 6 h, the thermal oil plants can reach the same or even lower LCOE as molten salt plants. For the Dubai site, the break-even point between VP1 and Solar Salt is at about 12 h of storage capacity, for Morocco at about 7 h, and for Dubai, about 14 h. The LCOE advantage of YaraMOST over Solar Salt is more pronounced for sites with lower annual DNI.

In Figure 6, LCOE is plotted versus capacity factor for each system, site, and thermal storage (TES) capacity. Each marker on the lines represents a certain storage capacity, from left to right: 6, 8, 10, 12, 15, and 18 h. From this plot, it becomes obvious that the molten salt plants need larger storage capacities to reach the same annual net electrical output for the same site. The results for Dubai show that a capacity factor (CF) of 0.7 (since the nominal power block size is identical for all plants, the same CF means also identical annual net

output) will be reached for the VP 1 system with 12 h TES capacity, while the Solar Salt systems need approximately 16 h and the YaraMOST plant needs about 13.5 h. In general, Figure 6 shows that the storage capacity should be about 1.5 to 3 h larger for molten salt systems to reach the same CF as VP1 systems at the same site. Our first hypothesis was that this is due to the additional heat required for freeze protection, which must be stored in the tanks and cannot be used for electricity production. But deeper analysis showed that freeze protection heat drawn from TES for one night for the molten salt systems is small compared to the thermal energy needed for 3 h of nominal power block (PB) operation (about 280 MWh for one night of freeze protection compared to 1033 MWh for 3 h of nominal PB operation). Therefore, this is only one part of the explanation. The plants using VP1 show larger solar fields compared to the plants using molten salts at the same site, and therefore they reach higher annual heat output, leading to higher annual electricity production. Due to higher TES costs, for VP1 plants, the optimal solar field size shifted toward larger fields.

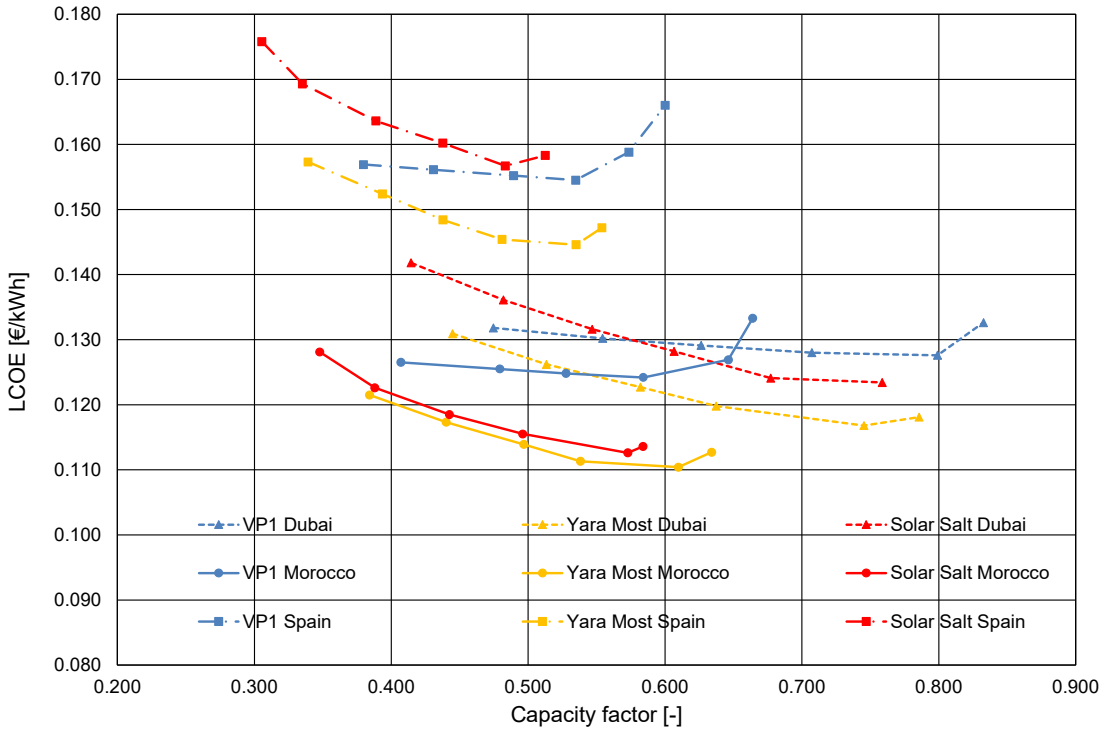

Figure 6. Results showing the LCOE versus the capacity factor for the lowest cost configurations.

From Figures 5 and 6, it is also obvious that increasing the storage capacity beyond 15 h will not lead to lower LCOE, since the additional capacity will not be used often during the typical operating year. The only exception is the plant using Solar Salt at Dubai, which shows the lowest LCOE for a TES capacity of 18 h.

Table 4 shows important results for all plants with 12 h of storage capacity. The plants at the Spanish site show about 30% larger solar fields compared to the plants located in Morocco, which is due to the lower annual DNI resource. The plants located in Dubai have about 50% larger solar fields compared to their pendants in Morocco. Due to the lower seasonal variability in Dubai, this additional mirror area pays off and leads to very high capacity factors. This larger solar field size for the plats at Dubai is also expressed by larger solar multiples, although all plants shown in Table 4 have the same power block size and the same TES capacity (equivalent to 12 full load hours). Table 4 shows that freeze protection is zero for the VP1 plants and very low for YaraMOST plants, while for Solar Salt plants, it is equivalent to about 5–8% of the annual heat produced by the solar field. A

considerable fraction (37–72%) of this freeze protection must be performed with external heat from natural gas or other energy carriers. Including a forecast for this freeze protection heat for several days could reduce this fraction of auxiliary heat.

Table 4. Detailed result comparison for the least LCOE plants with 12 h storage capacity (freeze protection: FP).

HTF	**VP1**			**YaraMOST**			**Solar Salt**			**Unit**
Site	**Morocco**	**Dubai**	**Spain**	**Morocco**	**Dubai**	**Spain**	**Morocco**	**Dubai**	**Spain**	
Annual DNI	2518	2026	2020	2518	2026	2020	2518	2026	2020	kWh/m²
Aperture area	1.768	2.678	2.273	1.515	2.273	1.970	1.439	2.273	1.970	km²
Solar multiple	2.74	4.15	3.52	2.57	3.86	3.34	2.52	3.98	3.45	-
Annual heat production	2221	2708	2042	1798	2148	1616	1620	1964	1462	GWh
FP heat from TES	0	0	0	0	0	0.1	51.4	28.8	67.7	GWh
FP heat from aux. firing	0	0	0	1.1	0	2.2	30.1	74.1	53.7	GWh
Net electricity production	767.6	929.3	702.7	707.3	837.5	631.9	651.9	797.1	575.2	GWh
LCOE	0.124	0.128	0.155	0.111	0.120	0.145	0.115	0.128	0.160	€/kWh
Capacity factor	58.4	70.7	53.5	53.8	63.7	48.1	49.6	60.7	43.8	-
Solar field efficiency	49.9	49.9	44.5	47.1	46.6	40.6	44.7	42.6	36.7	%
Net electricity/annual heat production	34.6	34.3	34.4	39.3	39.0	39.1	40.2	40.6	39.3	%

As mentioned in Section 2.1, using the arithmetic mean temperature between the inlet and outlet for the solar field simulation would lead to an underestimation of heat losses. The least LCOE plant configurations shown in Table 3 have been used to calculate the annual net electrical output of these plants using the simple solar field model in greenius with the arithmetic mean temperature approach. The result was that this leads to an overestimation of net electrical yield of about 1–3% for VP1, 6–10% for YaraMOST, and 11–16% for Solar Salt. Since all other parameters are kept the same for each site and HTF, the LCOE will be underestimated by the same ratio. The highest deviations were observed for the Spanish plants, which are operated more often in lower part load operation hours, which is expressed by their low capacity factors.

In Figure 7, the simulation results for 2 days in April for the plants using Solar Salt, 12 h of TES, and located in Morocco are plotted. The purple line represents the direct irradiation on the collectors, and the green line represents the usable heat delivered by the solar field. The offset in the morning between both lines is due to solar field heat-up, and the step in the green line in late afternoon hours represents the instant of time when the storage is fully charged and parts of the solar field must be defocused. The yellow line represents the calculated solar field outlet temperature with a heat-up period in the morning and cool-down after sunset. The blue line shows the required freeze protection, which can be conducted using warm salt from TES for these 2 days. The heat capacity of the solar field is sufficient to keep the outlet temperature above 270 °C from sunset until 2:00 in the morning. After this time, additional heat from the TES must be used to keep the temperature above this value and prevent the HTF from freezing.

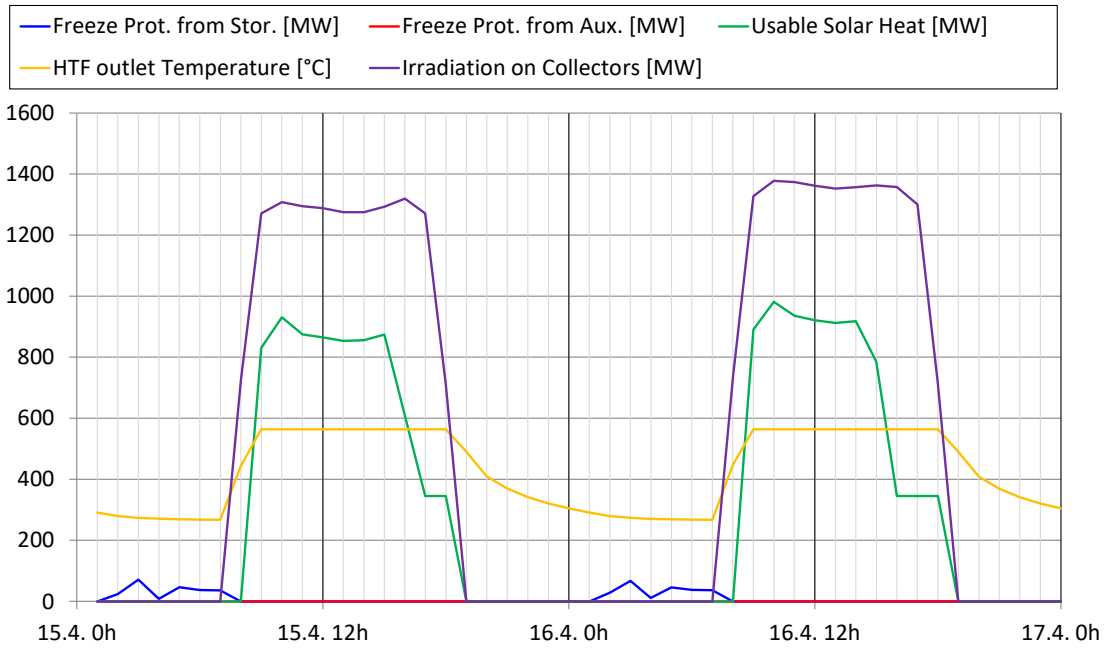

Figure 7. Simulation results for the Solar Salt plant at the Morocco site.

4. Conclusions

This study shows that parabolic trough plants using molten salt as heat transfer fluid and storage mediums have the potential to reach lower levelized cost of energy (LCOE) compared to plants using thermal oil as heat transfer fluid, particularly for plants with large storage capacities. For this analysis, typical plant setups leading to capacity factors from 0.3 to 0.8 were investigated. The ternary salt ($Ca(NO_3)_2$-KNO_3-$NaNO_3$, 42–43-15 wt.%, commercial names: Hitec XL or YaraMOST) leads to lower LCOE than Solar Salt due to the lower freezing temperature and the lower maximal solar field temperature. For the high DNI site in Morocco, both salt configurations clearly outperform the VP1 configuration with a benefit for the ternary salt compared to Solar Salt. The results indicate that Solar Salt can outperform the ternary salt for very large storage capacities beyond 18 h. For the sites in Dubai and Spain, the ternary salt yields lower LCOE than VP1, with increasing benefits as storage size becomes larger. LCOE for plants using Solar Salt at these two sites becomes lower than for plants using VP1 for storage capacities of more than 12 h. However, the ternary salt is still better than Solar Salt.

Due to the high operating temperature in molten salt solar fields, it is important to consider the real temperature profile along the parabolic trough loops in the performance model. Using just the mean arithmetic temperature between solar field inlet and outlet for heat loss calculations may lead to the underestimation of heat losses and the overestimation of annual electrical yield of up to 16%, depending on heat transfer fluid, site, and solar field size.

Freeze protection of the molten salt plants should be conducted primarily with heat from the thermal storage. The ternary salt YaraMOST needs only a small amount of freeze protection, while the plants using Solar Salt may need up to 8% of the annual heat collected by the solar field for freeze protection.

Author Contributions: Conceptualization: T.H., M.K.W. and J.D.; methodology: T.H., M.K.W. and J.D.; software: J.D.; writing—original draft preparation, J.D.; writing—review and editing: T.H. and M.K.W. All authors have read and agreed to the published version of the manuscript.

Funding: This research was funded by the Germany Federal Ministry for Economic Affairs and Climate Action, grant number 03EE5028B.

Data Availability Statement: The data presented in this study are available on request from the corresponding author due to copyright restrictions on some of the datasets.

Conflicts of Interest: The authors declare no conflicts of interest. The funders had no role in the design of the study; in the collection, analyses, or interpretation of data; in the writing of the manuscript; or in the decision to publish the results.

Abbreviations

CAPEX	Capital expenditure
CF	Capacity factor
CST	Concentrated solar thermal
DNI	Direct normal irradiance
EPC	Engineering, procurement, and construction
FP	Freeze protection
HTF	Heat transfer fluid
LCOE	Levelized cost of electricity
O&M	Operations and maintenance
PB	Power block
TES	Thermal energy storage

References

1. Kearney, D.; Kelly, B.; Herrmann, U.; Cable, R.; Pacheco, J.; Mahoney, R.; Price, H.; Blake, D.; Nava, P.; Petrovitza, N. Engineering aspects of a molten salt heat transfer fluid in a trough solar field. *Energy* **2004**, *29*, 861–870. [CrossRef]
2. Falchetta, M.; Liberati, G.; Consoli, D.; Mallogi, S.; Mazzei, D.; Crescenzi, T. Commissioning of the Archimede 5 MW molten salt parabolic trough solar plant. In Proceedings of the 16th SolarPACES Conference, Perpignan, France, 21–24 September 2010.
3. Krüger, D.; Detzler, R.; Schmitz, M.; Jung, C.; Bonk, A.; Hanke, A.; Horta, P.; Martins, P.; Torabzadegan, M.; Stengler, J. Operating parabolic troughs with molten salt: Solar field optimization and ternary salt properties. In Proceedings of the 28th International Solar PACES Conference, Abuquerque, NM, USA, 27–30 September 2022. [CrossRef]
4. Dicke, N.; Meyer-Grünefeldt, M.; Wittmann, M.; Stengler, J.; Horta, P.; Martins, P.; Stefan, C. Demonstration of 3.5 MWth Parabolic Trough with Ternary Molten Salt at the Évora Molten Salt Platform. In Proceedings of the 28th International Solar PACES Conference, Albuquerque, NM, USA, 27–30 September 2022. [CrossRef]
5. World's First Utility-Scale Molten Salt Fresnel CSP Plant Connects to Chinas Grid. Available online: https://www.solarpaces.org/worlds-first-utility-scale-molten-salt-fresnel-csp-plant-connects-to-chinas-grid/ (accessed on 24 September 2024).
6. Ruegamer, T.; Kamp, H.; Kuckelkorn, T.; Schiel, W.; Weinrebe, G.; Nava, P.; Riffelmann, K.J.; Richert, T. Molten salt for parabolic trough applications: System simulation and scale effects. *Energy Proceedia* **2014**, *49*, 1523–1532. [CrossRef]
7. Pan, C.A.; Guedez, R.; Dinter, F.; Harms, T.M. A techno-economic comparative analysis of thermal oil and molten salt parabolic trough power plants with molten salt solar towers. *AIP Conf. Proc.* **2019**, *2126*, 120014. [CrossRef]
8. Shininger, R.; Price, H. SMART: Simplified Melting and Rotation-Joint Technology; Technical Report; Solar Dynamics LLC, 1105 W. 11th Ct., Broomfield, CO 80020, 2021. Available online: https://www.osti.gov/biblio/1882508 (accessed on 23 September 2024).
9. Giaconia, A.; Tizzoni, A.C.; Sau, S.; Corsaro, N.; Mansi, E.; Spadoni, A.; Delise, T. Assessment and perspectives of heat transfer fluids for CSP applications. *Energies* **2021**, *14*, 7486. [CrossRef]
10. Delise, T.; Tizzoni, A.C.; Menale, C.; Telling, M.T.F.; Bubbico, R.; Crescenzi, T.; Corsaro, N.; Sau, S.; Licoccia, S. Technical and economic analysis of a CSP plant presenting a low freezing ternary mixture as storage and transfer fluid. *Appl. Energy* **2020**, *265*, 114676. [CrossRef]
11. Starke, A.R.; Cardemil, J.M.; Bonini, V.R.; Escobar, R.; Castro-Quijada, M.; Videla, Á. Assessing the performance of novel molten salt mixtures on CSP applications. *Appl. Energy* **2024**, *359*, 122689. [CrossRef]
12. Gallardo, F.; Guerreiro, L.; Gomes, J. Exergoeconomic Comparison of Conventional Molten Salts versus Calcium Based Ternary Salt as Direct HTF-TES In CSP Parabolic Troughs Collectors. In Proceedings of the ISES Solar World Congress, SWC 2019 and IEA SHC International Conference on Solar Heating and Cooling for Buildings and Industry 2019, SHC 2019, Santiago, Chile, 4–7 November 2019. [CrossRef]

13. Fahir, Z.; Mukhutar, M.F.; Shad, M.R.; Asghar, F.; Shahzad, M.; Asim, M.; Hasn, M.; Mujtaba, M.A.; Siddiqi, S.H.; Ali, T.; et al. Techno-Economic Analysis and Optimization of 50 MWe Linear Fresnel Reflector Solar Thermal Power Plant for Different Climatic Conditions. *Case Stud. Therm. Eng.* **2024**, *61*, 104909. [CrossRef]
14. Kannaiyan, S.; Bokde, N.D. Performance of Parabolic Trough Collector with Different Heat Transfer Fluids and Control Operation. *Energies* **2022**, *15*, 7572. [CrossRef]
15. Zurita, A.; Mata-Torres, C.; Valenzuela, C.; Felbol, C.; Cardemil, J.M.; Guzman, A.M.; Escobar, R.A. Techno-Economic Evaluation of a Hybrid CSP + PV Plant Integrated with Thermal Energy Storage and a Large-Scale Battery Energy Storage System for Base Generation. *Sol. Energy* **2018**, *173*, 1262–1277. [CrossRef]
16. Iñigo-Labairu, J.; Dersch, J.; Hirsch, T.; Giuliano, S.; Loevenich, M.; Córdoba, D. Techno-Economic Evaluation of CSP–PV Hybrid Plants with Heat Pump in a Temperature Booster Configuration. *Energies* **2024**, *17*, 2634. [CrossRef]
17. Gedle, Y.; Schmitz, M.; Gielen, H.; Schmitz, P.; Herrmann, U.; Boura, C.T.; Mahdi, Z.; Caminos, R.A.C.; Dersch, J. Analysis of an Integrated CSP-PV Hybrid Power Plant. *AIP Conf. Proc.* **2022**, *2445*, 030009. [CrossRef]
18. Turchi, C.S.; Ma, Z.; Neises, T.W.; Wagner, M. Thermodynamic Study of Advanced Supercritical Carbon Dioxide Power Cycles for Concentrating Solar Power Systems. *J. Sol. Energy Eng. Trans. ASME* **2013**, *135*, 041007. [CrossRef]
19. Linares, J.; Martín-Colino, A.; Arenas, E.; Montes, M.J.; Cantizano, A.; Pérez-Domínguez, J.R. A Novel Hybrid CSP-PV Power Plant Based on Brayton Supercritical CO_2 Thermal Machines. *Appl. Sci.* **2023**, *13*, 9532. [CrossRef]
20. Guccione, S.; Guedez, R. Techno-Economic Optimization of Molten Salt Based CSP Plants Through Integration of Supercritical CO_2 Cycles and Hybridization with PV and Electric Heaters. *Energy* **2023**, *283*, 128528. [CrossRef]
21. Greenius Website. Available online: https://www.dlr.de/en/sf/research-and-transfer/research-services/simulation-and-profitability-assessment/greenius-software-tool (accessed on 22 October 2024).
22. Janotte, N.; Lüpfert, E.; Pottler, K.; Schmitz, M. Full parabolic trough qualification from prototype to demonstration loop. *AIP Conf. Proc.* **2017**, *1850*, 020010. [CrossRef]
23. Bonk, A.; Sau, S.; Uranga, N.; Hernaiz, M.; Bauer, T. Advanced heat transfer fluids for direct molten salt line-focusing CSP plants. *Prog. Energy Combust. Sci.* **2018**, *67*, 69–87. [CrossRef]
24. Riffelmann, K.-J.; Lüpfert, E.; Richert, T.; Nava, P. Performance of the Ultimate Trough® collector with molten salt as heat transfer fluid. In Proceedings of the 18th SolarPACES Conference, Marrakech, Morocco, 11–14 September 2012.
25. Burkholder, F.; Kutcher, C. *Heat Loss Testing of Schott's 2008 PTR70 Parabolic Trough Receiver*; Technical Report NREL/TP-550-45633; National Renewable Energy Lab.: Golden, CO, USA, 2009.
26. Dersch, J.; Paucar, J.; Schuhbauer, C.; Schweitzer, A.; Stryk, A. *Blueprint for Molten Salt CSP Power Plant Final Report of the Research Project "CSP-Reference Power Plant" No. 0324253*; Institute of Solar Research: Cologne, Germany, 2021; Available online: https://elib.dlr.de/141315/ (accessed on 23 September 2024).